Indian Statistical Institute

Certificate of Approval

This is to certify that the thesis entitled "Reconstruction of discrete sets from projections with applications to computerized tomography" by Prakash Kumar Patra towards partial fulfillment for the degree of M Tech in Computer Science at Indian Statistical Institute, Kolkata, embodies the work done under my supervision.

(Bhargab B Bhattacharya)

ACMU, Indian Statistical Institute

Date Kolkata

ACKNOWLEDGMENT

I take this opportunity to thank Prof. Bhargab B Bhattacharya, Advanced Computing and Microelectronics Unit, ISI Kolkata for his valuable guidance and inspiration. His pleasant and encouraging words have always kept my spirit up.

Finally I would like thank all my class mates, my wife Dr Nivedita Karmee and my son Aditya for their support and motivation to complete this project.

Prakash Kumar Patra

M. Tech(CS)
Roll No.CS-0802

Date :

Indian Statistical Institute

Kolkata

Abstract

This thesis presents a reconstruction technique for computing a (0, 1) matrix uniquely from the projection information along rays shot from suitable projection angles. For reconstruction, we impose no restriction on any geometrical properties of the matrix. We determine a suitable set of projection directions for unambiguous reconstruction of a matrix from its projections.

The worst case time complexity of reconstruction is $O(m.n.(m+n))$ where m is the number of rows and n is the number of columns.

This work also presents a technique to identify the components (maximal 4 connected subsets) of a discrete set if the set to be reconstructed is canonical, from the projections along different angles. The projection angles may be as

$\tan^{-1}2$, $\tan^{-1}1/2$, $\tan^{-1}3$, $\tan^{-1}1/3$

The worst case time complexity for Identification of components is $O(m^2.n^2)$.

Contents

Chapter 1

1. Introduction

The main task of Discrete Tomography (DT) is to reconstruct discrete sets from a few projections. The number of projections should be minimized so as to keeps exposure to 'X' ray in the body tissue within acceptable limits.

The main problem of reconstruction is when this projection information fail to recreate the original matrix uniquely, i.e., there may be many different discrete sets with the same set of projections. One approach to remove ambiguity to restrict the reconstruction to a class of discrete sets which satisfy some geometrical properties. The ambiguity can also be reduced by having some prior knowledge about the matrix to be reconstructed.

The reconstruction of horizontally and vertically convex (shortly, hv-convex) discrete sets using only two projections is known to be NP-hard [6] . However, if the set is connected, then polynomial time reconstruction is possible [7,8,9,10]

Several algorithms have been proposed for solving the reconstruction problem in the class HV_4 of hv-convex polyminoes in polynomial time using the horizontal and vertical projections, among them the fastest one has a worst case time complexity of $O(mn.min(m^2,n^2))$ where m and n are the number of rows and columns of the matrix respectively [11,12,13] .One of the main difficulties in this task is that in certain cases the projections do not uniquely determine the binary matrix [5]. If the sizes of the components are small then the probability of error is large for forming discrete sets.

In this work it is shown that the large components of any discrete set can be reconstructed without ambiguity by choosing suitable projection angles. It is also shown that all the ray measurements of a view are not necessary. So the actual ray exposure on the volume/area is small.

As if A is the tissue area represented by the matrix then the average number of time expose of area by 'X' ray for 7*8 and 5*4 matrix are 2.545*A and 1.428*A respectively for reconstruction of matrix . The exposed area can further be reduced by decreasing the thickness of the ray.

Matrices of large size can also be reconstructed without ambiguity with reduced exposed area by reducing the width of the ray and by properly choosing exposure directions.

The worst case time complexity of reconstruction is O(m.n.(m+n)), where m is the number of rows and n is the number of columns.

It may be noted that the time complexity for reconstructing canonical hv-convex discrete sets becomes $O(m^3n^3.\min\{m^2,n^2\})$ if an earlier algorithm[3] is used.

We show that If the discrete set to be reconstructed is canonical, then the components can be identified by taking projections along a few angles 'ɵ' = $\tan^{-1}2$, $\tan^{-1}1/2$, $\tan^{-1}3$ & $\tan^{-1}1/3$. It also shown that the worst case time complexity is $O(m^2n^2)$.

The organization of the thesis is the following.

Chapter2 and Chapter3 discuss preliminaries of computerized tomography and matrix representation.

Chapter 4 address the problem of ambiguity in reconstructing discrete sets from projections.

Chapter 5 demonstrates the reconstruction strategy that guarantees uniqueness from various angular projections.

Chapter 6 presents identification of components of hv-convex canonical discrete sets with projection of different angles.

CHAPTER 2

2. Preliminaries

2.1 First generation CT Basic Principle:

It is imagined that the subject to be scanned as being divided into axial slices. The X-ray beam to be used was collimated down to a narrow (pencil-width) beam of X-rays. The size of the beam is generally 3mm within the plane of the slice and 13mm width perpendicular to the slice(along the axis of the subject) In fact, it is the beam width that typically specifies the slice thickness to be imaged. The X-ray tube is rigidly linked to an X-ray detector located on the other side of the subject. Together the tube and the detector scan across the subject, sweeping the narrow X-ray beam through the slice.

Translation: This linear transverse scanning motion of the tube and the detector across the subject is referred to as a translation.

Ray: The X-ray beam path through the subject corresponding to each measurement is called a ray.

View: The set of measurements made during the translation and their associated rays is a view. Now a days scanners have 750 rays per view. After completion of the translation, the tube-detector assembly is rotated around the subject and translation is repeated to collect another view. Today's scanners may typically collect 1000 or more views over 360 degree.

Fig : 1

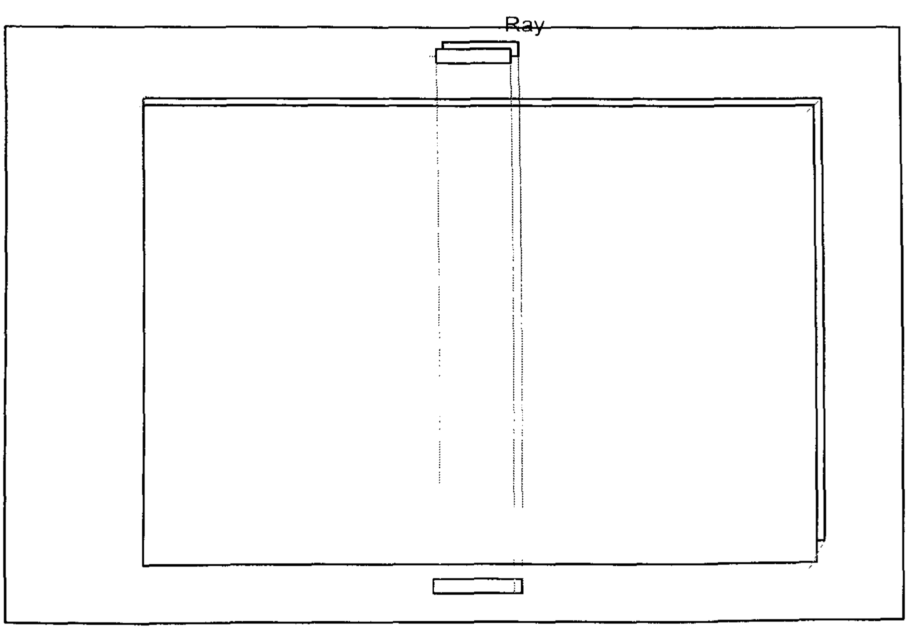

C T Image Reconstruction:

It is imagine that the slice is divided into a matrix of 3-dimensional rectangular boxes (voxel) of material(tissue).

Reconstruction Matrix

If translation cover 250 mm and if the scan area is divided into a matrix of 250 rows and 250 columns with each voxel of 1mm * 1mm. This matrix is referred to as reconstruction matrix.

CT image reconstruction is to determine how much attenuation of the narrow X-ray beam occurs in each voxel of the reconstruction matrix.

These calculated attenuation values are then represented as gray level in a 2-dimensional Image of the slice.

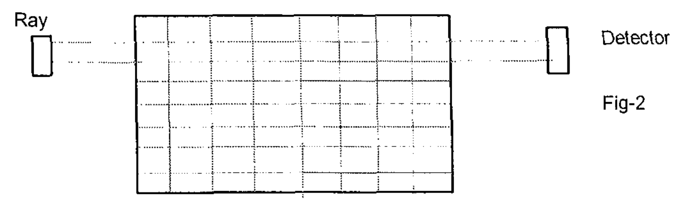

Fig-2

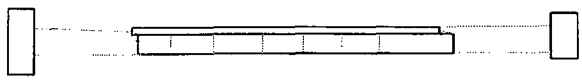

Fig -3

Representation of attenuation as pixel value

N_0=X-ray intensity entering the row of voxels

N_i= Detector measured intensity

W_i = Path length of the ray

μ_i = Attenuation coefficient

N_1 = Intensity exiting the first voxel (attenuation = μ_1)

$N_1 e^{-(w2\mu2)} = N_0 e^{-(w1\mu1)}$

$N_2 = N_1 e^{-(w2\mu2)} = N_0 e^{-(w1\mu1)} e^{-(w2\mu2)}$

$N_i = N_0 e^{-(w1\mu1)} e^{-(w2\mu2)} \ldots\ldots\ldots\ldots e^{-(wn\mu n)}$

Or $-\ln(N_i / N_0) = W_1 \mu_1 + W_2 \mu_2 + W_1 \mu_1 \ldots\ldots\ldots\ldots + W_n \mu_n$

Each term $w_i\mu_i$ represents the attenuation occurring within voxel

which is designated as u_i.

$N'_i = u_1 + u_1 + u_2 + u_3 + \ldots\ldots\ldots\ldots\ldots\ldots u_n$

2. Representation of the projection value [1].

W_{ji} for this cell = area of ABCD / r^2

f_j denote the constant value in the jth cell which depends on the attenuation value .

N is the total number of cells =$(f_n)^2$

Let p_i be the projection of ith ray .

$\sum W_{ji} f_j = P_i$ i= 1,2,3 .....M

(j=1 to j=N)

Where M is the total number of rays (in all the projections)

Knowing f_j (denote the constant value in the jth cell) and considering a threshold value the binary image can be constructed. If the value of the constant is greater than the threshold value then '1 'is assigned to the pixel. If the value is less than threshold value then '0' is assigned to the pixel.

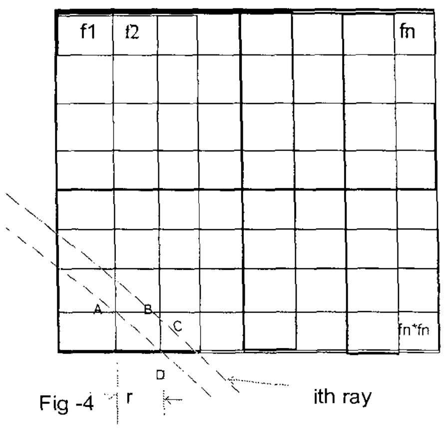

Fig -4

Chapter 3

3. Some Definitions

he 4-connected sets are called polyominoes **4-connected :** A discrete set F is 4-connected if for any two distinct positions P,Q ∈ F. There exists a sequence of distinct position

$(i_0,j_0)=P.........(i_k,j_k)=Q$ such that $(i_l,j_l) \in F$ and $| i_l - i_{l+1} | + | j_l - j_{l+1} | = 1$

for each $l=0,1$ ....(k-1)

8-connected A discrete set F is 8-connected if for any two distinct positions P, Q ∈ F.

There exists a sequence of distinct position $(i_0,j_0)=P.........(i_k,j_k)=Q$ such that $(i_l,j_l) \in F$

and $| i_l - i_{l+1} | + | j_l - j_{l+1} | \leq 2$ for each $l=0$,..............................(k-1)

Polyominoes T

Components: If a discrete set is not 4-connected then it can be partitioned

(in a uniquely determined way) into maximum 4-connected subsets which are called components of the discrete set.

Canonical (anti-canonical)

The discrete set is canonical (anti-canonical) if it consists of just one component or the smallest containing rectangles of the components are connected to each other with their bottom –right and upper left (bottom-left and upper –right) corners.

hv-convex A discrete set is called hv-convex if all the rows and columns of the set are 4-connected.

0	1	1	0	0	0
0	1	1	1	0	0
1	1	1	1	0	0
1	1	1	1	1	1
0	1	1	1	1	0

hv-convex 4 connected

1	1	1	0	0	0
1	1	1	1	0	0
0	1	1	1	0	0
0	0	0	0	1	1
0	0	0	0	1	1
0	0	0	0	1	0

hv-convex 8 connected

0	1	1	0	0	0
0	1	1	1	0	0
1	1	0	0	0	0
0	0	0	0	1	1
0	0	0	0	1	0

hv-convex canonical

0	1	0	0	0	0
1	1	0	0	0	0
0	0	0	0	1	0
0	0	0	0	1	1
0	0	1	1	0	0

general hv-convex

Fig- 5

Chapter 4

4. Discussion about Unambiguous and Ambiguous cases

4.1 : Unambiguous Cases: This is the case where reconstruction of the matrix is unique. This is possible if there is no (1, 0) and (0, 1) pair forming a sub-matrix explained below in the discrete set.

Explanation : Let there be an m*n matrix, where 'I' & 'j' are any integer from 1 to m and 'k' and 'I' are any integer from 1 to n, where R_i and R_j are ith and jth row respectively and

C_k and C_l combinations as given below .

	C_k	C_l	
R_i	0	1	where (i != j) and (k != l)
R_j	1	0	

and

	C_k	C_l	
R_i	1	0	where (i != j) and (k != l)
R_j	0	1	

Example: Unambiguous cases

0	1	1	0	0	0
1	1	1	1	0	0
0	0	0	1	0	0
0	0	0	1	1	1
0	0	0	0	0	1
0	0	0	0	0	1

Fig- 6(a)

0	1	1	0	0	0
0	1	1	1	0	0
1	1	1	1	0	0
0	0	0	0	1	1
0	0	0	0	0	1
0	0	0	0	1	1

Fig – 6(b)

4.2 : Ambiguity of reconstruction of discrete sets.

Generally ambiguity of reconstruction of matrix occurred due to presence of (1,0) and (0,1) combination as shown in 4.1 .

Examples of ambiguous cases are given below .

1	0	1	1	1	0
1	1	1	1	0	1
1	0	1	1	1	1
1	1	0	1	0	1
0	0	1	1	1	0
0	0	0	0	1	1

Fig – 7(a)

1		0	0	1	0
0	1	0	1	0	1
0	0	0	1	1	1
0	1	0	1	0	1
1	0	0	0	1	0
1	1	1	1	0	1

Fig – 7(b)

Reconstruction of such type of matrices is not unique as with the same horizontal and vertical projections , It may give many matrices .

4 .3 On the Ambiguity of Reconstructing hv-convex Binary Matrices with Decomposable Configurations by Pr. Peter Balazs .[5]

Preliminaries : A discrete set with the smallest containing discrete rectangle (SCDR) of size

m*n can be represented by a binary matrix $F=(f_{ij})_{m*n}$.

Size of discrete set: It is m*n.

Where m= number of rows, n = number of column .

Number of elements : It is the number of '1' present in the matrix .

Different projections are:

Horizontal projection = H(F)

$H(F) = H = (h_1, h_2, \text{-----} h_m)$.

$h_i = \sum f_{ij}$ (i= 1,2,..........m)

for j is from 1 to n

Vertical projection V(F)

$V(F) = V = (v_1, \ldots\ldots\ldots\ldots v_n$

$v_{ij} = \sum f_{ij}$ (j= 1,2,..........n)

for i is from 1 to m .

Diagonal projection D(F) ;

$D = (d_1, d_2, \text{-----} d_{m+n-1})$

$d_k = \sum f_{ij}$ (K= 1,2,..........m +n – 1)

i+ (n-j) = K

Anti-diagonal projection A(F) ;

$A(F) = A = (a_1, a_2, \text{----- ---} a_{m+n-1})$

$a_k = \sum f_{ij}$ (K= 1,2,.......m +n- 1)

i+ (n-j) = K

Projection: With negative result

Theorem: 1 **Three Projections:** For some vectors H , V , D there can be exponentially many hv convex decomposable binary matrices with the same horizontal, vertical, and diagonal projections H , V , D respectively.

$$M = \begin{matrix} 1 & 0 & 0 \\ 0 & 1 & 1 \\ 0 & 1 & 0 \end{matrix} \qquad M' = \begin{matrix} 0 & 1 & 0 \\ 1 & 1 & 0 \\ 0 & 0 & 1 \end{matrix}$$

Remarks: We get the same result replacing the diagonal projections with the anti-diagonal projections.

Four Projections: The reconstruction of a discrete sets from four projection is NP –hard.

Further the number of hv-convex discrete sets having the same four projections can be extremely large .

$$M = \begin{matrix} 0 & 0 & 1 & 0 \\ 1 & 0 & 0 & 0 \\ 0 & 0 & 0 & 1 \\ 0 & 1 & 0 & 0 \end{matrix} \qquad M' = \begin{matrix} 0 & 1 & 0 & 0 \\ 0 & 0 & 0 & 1 \\ 1 & 0 & 0 & 0 \\ 0 & 0 & 1 & 0 \end{matrix}$$

4.4: **Table 1**:

The number of hv-convex polyominoes in the test data sets that are not uniquely determined by two, three, and four projections. (Each data set consisted of 5000 discrete sets with same size)

Size n × n	H, V	H, V, D	H, V, A	H, V, D, A
4 × 4	1393	40	52	18
5 × 5	1442	33	36	16
7 × 7	967	13	8	2
10 × 10	586	4	6	1
20 × 20	312	2	1	1
40 × 40	210	1	0	0
60 × 60	162	1	0	0
80 × 80	148	0	0	0
100 × 100	171	0	0	0

Chapter 5

5 : Procedure for reconstruction of discrete set with projections of different angles.

5.1 Table: 1 Matrix with size different projection angles

Sl No	Maximum size of the matrices that can be reconstructed	Different projection angles required
1	4*5 or 5*4	$\theta = \tan^{-1}1$, $\theta = \tan^{-1}2$, $\theta = \tan^{-1}1/2$
2	8 * 7 or 7 * 8	$\theta = \tan^{-1}2$,$\theta = \tan^{-1}1/2$ $\theta = \tan^{-1}3$, $\theta = \tan^{-1}1/3$
4	19*20 or 20*19	$\theta = \tan^{-1}1$,$\theta = \tan^{-1}2$,$\theta = \tan^{-1}1/2$ $\theta = \tan^{-1}3$, $\theta = \tan^{-1}1/3$,$\theta = \tan^{-1}2/3$, $\theta = \tan^{-1}3/2$, $\theta = \tan^{-1}4$, $\theta = \tan^{-1}1/4$

5.2 Procedure for small size matrix:

Projection is started from the corner of the matrix as shown in the figure-7(a)

As shown in the figure -7(a) the angle of the 1st ray is $\tan^{-1}1$.

With the projection value of the ray we can get the pixel value of the the pixel numbered 1 , as this is the only unknown pixel value of that ray .

Similarly we can get the value of pixel numbered 1' on the other corner of the matrix .Next in the figure-9(b), it is shown for two ray projection for an angle $\theta = \tan^{-1}2$, $\theta = \tan^{-1}1/2$. One ray covers pixel 1 and 2. As pixel value of 1 is known the pixel value of 2 can be found. Another ray covers pixel 1 and 3. As pixel value of 1 is known the pixel value of 3 can be found from the projection value .Similarly in the other corner the pixel number 2' and 3' can be found. In this way if we proceed we can get all the pixel values of the matrix. There is limit of the maximum size of the matrix for the projection having angles as shown in the Table-1.

5.3 Procedure for higher size matrix: In this case the thickness of rays should be decreased by considering the limit of 'X' ray exposures. Then with the same procedure as above one should proceed. But when we will be unable to proceed then we have to decide suitable projection angle so that the ray covers single unknown pixel with other known pixels.

We may consider the projection angles as $\Theta = \tan^{-1}3/4$, $\Theta = \tan^{-1}4/3$, $\Theta = \tan^{-1}4/5$,

$\Theta = \tan^{-1}5/4$, $\Theta = \tan^{-1}1/4$, $\Theta = \tan^{-1}4$ so on.

5.4 Rays size

For projection $\Theta = \tan^{-1}2$, for convenience, the rays should be such that they cover 1/2 of the pixels of upper side.

For projection $\Theta = \tan^{-1}1/2$, each ray covers 1/2of the pixels of the left side.

For projection $\Theta = \tan^{-1}3$ for convenience, the rays should be such that it cover 1/3 of the pixel of upper side.

For projection $\Theta = \tan^{-1}1/3$, each ray covers 1/3 of the pixels on the left side. these are shown in the figure 8.

For projection $\Theta = \tan^{-1}3/2$ for convenience, the rays should be such that it cover 2/3 of the pixel of upper side.

For projection $\Theta = \tan^{-1}2/3$, each ray covers 2/3 of the pixels on the left side. these are shown in the figure 8.

If we take higher sized ray then unnecessary overlapping of rays will take place.

We can also take rays of smaller size as per image construction.

5.5 Calculation of ray exposed area: As per the ray size the number of rays required to cover the entire area is given below for the projection angle 'Θ'. Let the size of the matrix is m*n.

(1) $\Theta = \tan^{-1}2$, Number of rays $N= 2*n + m$.

(2) $\Theta = \tan^{-1}1/2$, Number of rays $N =2*m +n$.

(3) $\Theta = \tan^{-1}3$, Number of rays $N=3*n + m$.

(4) $\Theta = \tan^{-1} 1/3$, Number of rays $N= n +3*m$.

(5) $\Theta = \tan^{-1}3/2$, Number of rays $N=ceil((3/ 2)*n) + m$.

(6) $\Theta = \tan^{-1}2 /3$, Number of rays $N= n +ceil((3/2)*m)$

Let N_m = minimum of N among the above projections used for measurement.

Let the tissue area represented by the matrix be A

Average cover area of a ray for each case = A_r = A/ number of rays.

As previously explained that to find a pixel value of matrix a ray value is required.

So the number of rays required for m*n matrix is = m*n.

Thus it is not required to take all the ray measurement of a view.

In the worst case, the average maximum exposed area = $m*n*(A/N_m)$

In case of large matrix the thickness of rays can be reduced to get less exposed area.
Example : (i) For matrix 7*8

The worst case average exposed area = A(average) .

A(average) = 7*8* A/(2*7+8) = 2.545*A .

(ii) For matrix 5*4

The worst case average exposed area = A(average) .

A(average) = 5*4* A/(2*5+4) = 1.428*A .

Note: The area can be further be reduced by decreasing the thickness of the rays.

5.6: Calculation of time complexity (worst case)

With each ray value one pixel value can be found.

Number of pixel = m* n

So number of rays required for detection of pixel value is m*n.

For each pixel maximum number of iteration required = (m +n)

So the time complexity is = m*n*(m + n)

Different projections with their rays

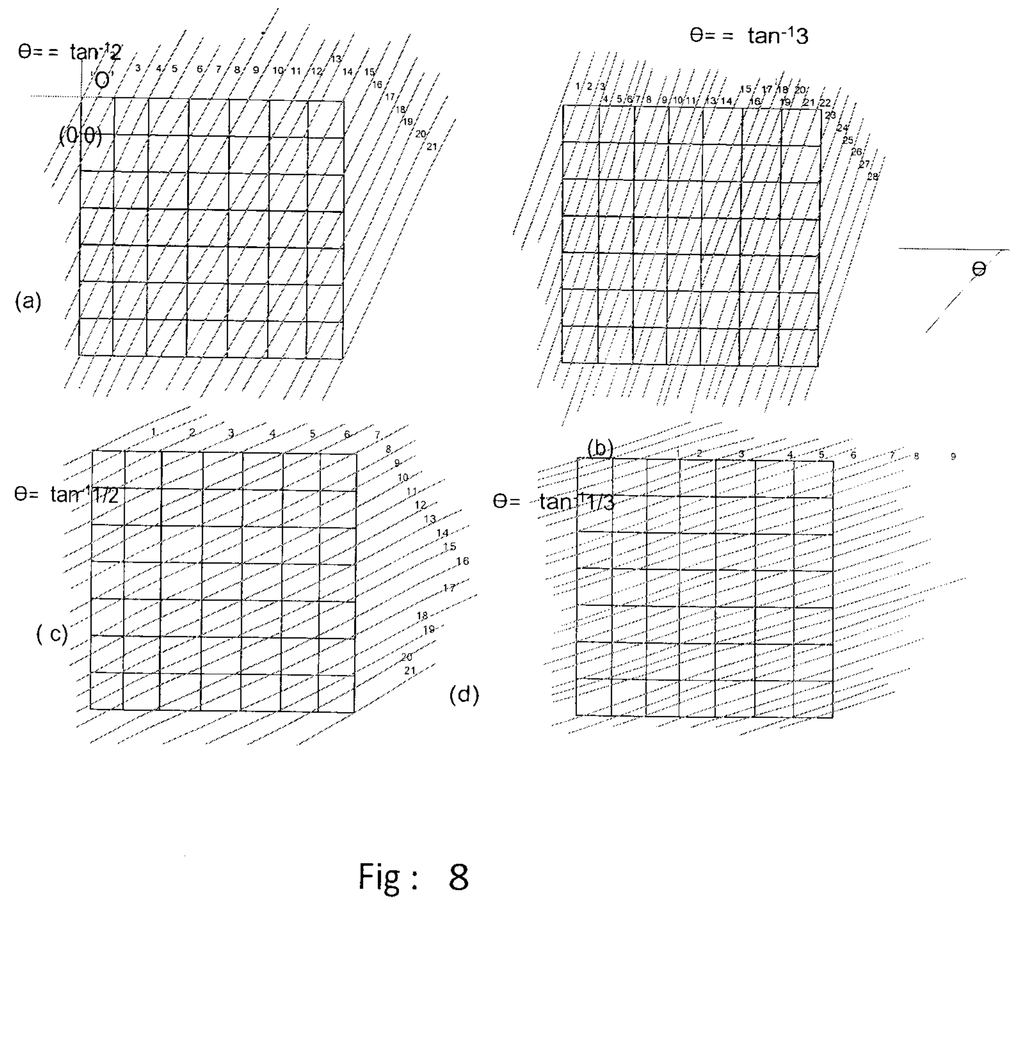

Fig : 8

5.7 Sequence of finding pixel number with projections

(i) Maximum size of matrices that can be uniquely determined by three projections θ =tan⁻¹1, θ =tan⁻¹2 , θ =tan⁻¹1/2 is 4*5 , 5*4 .

(a)

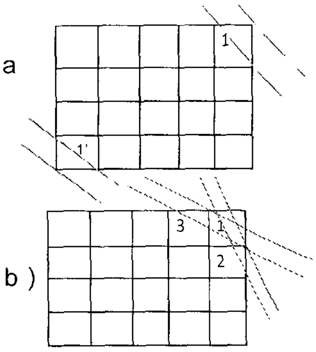

(b)

(c)

7'	8	5	3	1
4'	9'	10	6	2
2'	6'	10'	9	4
1'	3'	5'	8'	7

(d)

7'	8	3	1
7'	10	6	2
4'	9'	9	4
2'	6'	10'	7
1'	3'	5'	8'

Fig - 9

θ

Order in which the pixel values are determined	Angle of projection	Location of pixel that can be calculated
1	$\theta = \tan^{-1}1$	1, 1'
2	$\theta = \tan^{-1}2$	2, 2'
3	$\theta = \tan^{-1}1/2$	3, 3'
4	$\theta = \tan^{-1}2$	4, 4'
5	$\theta = \tan^{-1}1/2$	5 , 5'
6	$\theta = \tan^{-1}1$	6, 6'
7	$\theta = \tan^{-1}2$	7, 7'
8	$\theta = \tan^{-1}1/2$	8 , 8'
9	$\theta = \tan^{-1} 2$	9, 9'
10	$\theta = \tan^{-1}1/2$	10, 10'

(ii) Maximum size of matrices that can be uniquely determined by four projections $\theta = \tan^{-1}2$, $\theta = \tan^{-1}1/2$, $\theta = \tan^{-1} 3$, $\theta = \tan^{-1}1/3$ is 8*7 , 7*8 .

18'	14	10	7	5	3	1
17'	23'	20	16	12	8	2
13'	22'	27	25	21	11	4
9'	19'	26'	28	24	15	6
6'	15'	24'	28'	26	19	9
4'	11'	21'	25'	27'	22	13
2'	8'	12'	16'	20'	23	17
1'	3'	5'	7'	10'	14'	18

Fig ; 10

Angle of projection	Location of pixel that can be calculated
$\theta = \tan^{-1}2$	1, 1'
$\theta = \tan^{-1}2$	2, 2'
$\theta = \tan^{-1}1/2$	3, 3'
$\theta = \tan^{-1}2$	4, 4'
$\theta = \tan^{-1}1/2$	5, 5'
$\theta = \tan^{-1} 3$	6, 6'
$\theta = \tan^{-1}1/3$	7, 7'
$\theta = \tan^{-1}2$	8, 8'
$\theta = \tan^{-1} 3$	9, 9'
$\theta = \tan^{-1}1/ 3$	10, 10'

Angle of projection	Location of pixel that can be calculated
$\theta = \tan^{-1}2$	11, 11'
$\theta = \tan^{-1}1/2$	12 , 12'
$\theta = \tan^{-1}3$	13, 13'
$\theta = \tan^{-1}1/3$	14, 14'
$\theta = \tan^{-1}2$	15 , 15'
$\theta = \tan^{-1} 1/2$	16, 16'
$\theta = \tan^{-1}3$	17, 17'
$\theta = \tan^{-1} 1/3$	18, 18 '
$\theta = \tan^{-1} 3$	19, 19'
$\theta = \tan^{-1}1/ 3$	20, 20'

Angle of projection	Location of pixel that can be calculated
$\theta = \tan^{-1}2$	21, 21'
$\theta = \tan^{-1} 3$	22, 22'
$\theta = \tan^{-1}1/3$	23, 23'
$\theta = \tan^{-1}2$	24, 24'
$\theta = \tan^{-1}1/2$	25, 25'
$\theta = \tan^{-1} 2$	26, 26'
$\theta = \tan^{-1}1/2$	27, 27'
$\theta = \tan^{-1}2$	28, 28

(iii) Maximum size of matrices that can be uniquely determined by five projections $\theta = \tan^{-1}1, \theta = \tan^{-1}2$, $\theta = \tan^{-1}1/2$ $\theta = \tan^{-1}3$, $\theta = \tan^{-1}1/3$ is 9*8 , 8*9 .

22'	23	19	14	10	7	5	3	1
18'	28'	29	25	21	16	12	8	2
13'	24'	32'	34	31	27	17	11	4
9'	20'	30'	35'	36	33	26	15	6
6'	15'	26'	33'	36'	35	30	20	9
4'	11'	17'	27'	31'	34'	32	24	13
2'	8'	12'	16'	21'	25'	29'	28	18
1'	3'	5'	7'	10'	14'	19'	23'	22

Fig ; 11

Angle of projection	Location of pixel that can be calculated
$\theta = \tan^{-1}2$	1, 1'
$\theta = \tan^{-1}2$	2, 2'
$\theta = \tan^{-1}1/2$	3, 3'
$\theta = \tan^{-1}2$	4, 4'
$\theta = \tan^{-1}1/2$	5, 5'
$\theta = \tan^{-1} 3$	6, 6'
$\theta = \tan^{-1}1/3$	7, 7'
$\theta = \tan^{-1}2$	8, 8 '
$\theta = \tan^{-1} 3$	9, 9'
$\theta = \tan^{-1}1/ 3$	10, 10'

Angle of projection	Location of pixel that can be calculated
θ =tan^{-1}2	11, 11’
θ =tan^{-1}1/2	12 , 12’
θ =tan^{-1}3	13 , 13’
θ =tan^{-1}1/3	14 , 14’
θ =tan^{-1}2	15 , 15’
θ =tan^{-1} 1/2	16 , 16’
θ =tan^{-1}1	17 , 17’
θ =tan^{-1} 3	18 , 18 ‘
θ =tan^{-1} 1/3	19 , 19’
θ =tan^{-1}2	20 , 20’
θ =tan^{-1}1/2	21, 21’
θ =tan^{-1} 3	22 , 22’
θ =tan^{-1}1/3	23 , 23’

Angle of projection	Location of pixel that can be calculated
θ =tan^{-1}3	24, 24’
θ =tan^{-1}1/3	25, 25’
θ =tan^{-1} 2	26, 26’
θ =tan^{-1}1/2	27, 27’
θ =tan^{-1}3	28, 28
θ =tan^{-1}1/3	29, 29’
θ =tan^{-1}2	30, 30’
θ =tan^{-1} 1/2	39, 39’
θ =tan^{-1} 3	32 , 32’
θ =tan^{-1} 2	33, 33 ‘
θ =tan^{-1} 1/2	34, 34’
θ =tan^{-1}2	35, 35’
θ =tan^{-1}1/2	36, 36’

(iv) Maximum size of matrices that can be uniquely determined by projections $\theta = \tan^{-1}1, \theta = \tan^{-1}$ $\theta = \tan^{-1}1/2, \theta = \tan^{-1}3$, $\theta = \tan^{-1}1/3, \theta = \tan^{-1}2/3$, $\theta = \tan^{-1}3/2$, $\theta = \tan^{-1}4$, $\theta = \tan^{-1}1/4$ is 19*20 , 20*19

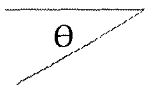

Fig - 12

1	3	5	7	10	14	18	20	25	31	37	41	48	56	67	79	83	93	103′
2	8	12	16	22	27	33	39	46	54	62	71	81	91	102	109	115	118′	92′
4	11	23	29	35	44	52	60	69	77	89	100	111	′117	120	124	131′	114	82′
6	15	28	42	50	58	65	75	37	48	113	122	130′	132	137	143′	123′	108′	78′
9	21	34	49	63	73	85	96	108a	128	135	142	145	149	154′	136′	119′	101′	66′
13	26	43	57	72	94	106	126	139	147	153	156	160	163′	148′	133′	116′	90′	55′
17	32	51	64	84	105	138	151	158	162	166	170	173″	154′	144″	129″	110′	80′	47′
19	38	59	74	95	125	150	164	168	172	175	176′	169′	155′	141′	121′	99′	70′	40′
24	45	68	86	107	140	157	167	177	178	180′	174′	165′	152′	134′	112′	88′	61′	36′
30	53	76	97	127	146	161	171	179	181	179′	171′	161′	146′	127′	97′	76′	53′	30′
36	61	88	112	134	152	165	174	180	178	177	167′	157′	140′	107′	86′	68′	45′	24′
40	70	99	121	141	155	169	176	175′	172′	168′	164′	150′	125″	95′	74′	59′	38′	19′
47	80	110	129	144	159	173	170′	166′	162′	158′	151′	138′	105′	84′	64′	51′	32′	17′
55	90	116	133	148	163	160′	156′	153′	147′	139′	126′	106′	94′	72′	57′	43′	26′	13′
66	101	119	136	154	149′	145′	142′	135′	128a′	108′	96′	85′	73′	63′	49′	34′	21′	9′
78	108	113	143	137′	132′	130′	122′	113′	48′	37′	75′	65′	58′	50′	42′	28′	15′	′6′
82	114	131	124′	120′	117′	111′	100′	89′	77′	69′	60′	52′	44′	35′	29′	23′	11′	4′
92	118	115′	109′	102′	91′	81′	71′	62′	54′	46′	39′	33′	27′	22′	16′	12′	8′	2′
103	93′	83′	79′	67′	56′	48′	41′	37′	31′	25′	20′	18′	14′	10′	7″	5′	3′	1′

(iv) Maximum size of matrices that can be uniquely determined by seven projections $\theta = \tan^{-1}1$, $\theta = \tan^{-1}2$, $\theta = \tan^{-1}1/2$, $\theta = \tan^{-1}3$, $\theta = \tan^{-1}1/3$, $\theta = \tan^{-1}3/2$, $\theta = \tan^{-1}2/3$, $\theta = \tan^{-1}4$, $\theta = \tan^{-1}1/4$ is 19*20 , 20*19 .

Angle of projection	Location of pixel that can be calculated
$\theta = \tan^{-1}2$	1, 1'
$\theta = \tan^{-1}2$	2, 2'
$\theta = \tan^{-1}1/2$	3, 3'
$\theta = \tan^{-1}2$	4, 4'
$\theta = \tan^{-1}1/2$	5, 5'
$\theta = \tan^{-1}3$	6, 6'
$\theta = \tan^{-1}1/3$	7, 7'
$\theta = \tan^{-1}1/2$	8, 8'
$\theta = \tan^{-1}3$	9, 9'
$\theta = \tan^{-1}1/3$	10, 10'

Angle of projection	Location of pixel that can be calculated
$\theta = \tan^{-1}2$	11, 11'
$\theta = \tan^{-1}1/2$	12, 12'
$\theta = \tan^{-1}3$	13, 13'
$\theta = \tan^{-1}1/3$	14, 14'
$\theta = \tan^{-1}2$	15, 15'
$\theta = \tan^{-1}1/2$	16, 16'
$\theta = \tan^{-1}3$	17, 17'
$\theta = \tan^{-1}1/3$	18, 18'
$\theta = \tan^{-1}4$	19, 19'
$\theta = \tan^{-1}1/4$	20, 20'
$\theta = \tan^{-1}3$	21, 21'

Angle of projection	Location of pixel that can be calculated
$\theta = \tan^{-1}1/3$	22, 22'
$\theta = \tan^{-1}2$	23, 23'
$\theta = \tan^{-1}4$	24, 24'
$\theta = \tan^{-1}1/4$	25, 25'
$\theta = \tan^{-1}3$	26, 26'
$\theta = \tan^{-1}1/3$	27, 27'
$\theta = \tan^{-1}2$	28, 28
$\theta = \tan^{-1}1/2$	29 , 29'
$\theta = \tan^{-1}4$	30, 30'
$\theta = \tan^{-1}1/4$	31, 31'
$\theta = \tan^{-1}3$	32, 32'
$\theta = \tan^{-1}1/3$	33, 33'

Angle of projection	Location of pixel that can be calculated
$\theta = \tan^{-1}2$	34, 34'
$\theta = \tan^{-1}1/2$	35, 35'
$\theta = \tan^{-1}4$	36, 36'
$\theta = \tan^{-1}1/4$	37, 37'
$\theta = \tan^{-1}3$	38, 38
$\theta = \tan^{-1}1/3$	39, 39'
$\theta = \tan^{-1}4$	40, 40'
$\theta = \tan^{-1}1/4$	41, 41'
$\theta = \tan^{-1}3/2$	42, 42'
$\theta = \tan^{-1}2$	43, 43'
$\theta = \tan^{-1}1/2$	44, 44'
$\theta = \tan^{-1}3$	45, 45'
$\theta = \tan^{-1}1/3$	46, 46'
$\theta = \tan^{-1}4$	47, 47'

Angle of projection	Location of pixel that can be calculated
$\theta = \tan^{-1} 1/4$	48 , 48'
$\theta = \tan^{-1} 3/2$	49, 49'
$\theta = \tan^{-1} 2/3$	50, 50'
$\theta = \tan^{-1} 2$	51, 51'
$\theta = \tan^{-1} 1/2$	52, 52'
$\theta = \tan^{-1} 3$	53, 53'
$\theta = \tan^{-1} 1/3$	54, 54'
$\theta = \tan^{-1} 4$	55, 55'
$\theta = \tan^{-1} 1/4$	56, 56'
$\theta = \tan^{-1} 3/2$	57, 57'
$\theta = \tan^{-1} 2/3$	58, 58'
$\theta = \tan^{-1} 2$	59, 59'

Angle of projection	Location of pixel that can be calculated
$\theta = \tan^{-1} 1/2$	60, 60'
$\theta = \tan^{-1} 3$	61, 61'
$\theta = \tan^{-1} 1/3$	62, 62'
$\theta = \tan^{-1} 3/2$	63, 63'
$\theta = \tan^{-1} 3/2$	64, 64'
$\theta = \tan^{-1} 2/3$	65, 65'
$\theta = \tan^{-1} 4$	66, 66'
$\theta = \tan^{-1} 1/4$	67, 67'
$\theta = \tan^{-1} 2$	68, 68'
$\theta = \tan^{-1} 1/2$	69, 69'
$\theta = \tan^{-1} 3$	70, 70'
$\theta = \tan^{-1} 1/3$	71, 71'
$\theta = \tan^{-1} 3/2$	72 , 72'
$\theta = \tan^{-1} 2/3$	73, 73'

Angle of projection	Location of pixel that can be calculated
$\theta = \tan^{-1} 3/2$	74, 74'
$\theta = \tan^{-1} 2/3$	75, 75'
$\theta = \tan^{-1} 2$	76, 76'
$\theta = \tan^{-1} 1/2$	77, 77'
$\theta = \tan^{-1} 4$	78, 78'
$\theta = \tan^{-1} 1/4$	79, 79'
$\theta = \tan^{-1} 3$	80, 80'
$\theta = \tan^{-1} 1/3$	81, 81'
$\theta = \tan^{-1} 4$	82, 82'
$\theta = \tan^{-1} 1/4$	83, 83'
$\theta = \tan^{-1} 3/2$	84, 84'
$\theta = \tan^{-1} 2/3$	85, 85'
$\theta = \tan^{-1} 3/2$	86, 86'
$\theta = \tan^{-1} 2/3$	87, 87'

Angle of projection	Location of pixel that can be calculated
$\theta = \tan^{-1} 2$	88, 88'
$\theta = \tan^{-1} 1/2$	89, 89'
$\theta = \tan^{-1} 3$	90, 90'
$\theta = \tan^{-1} 1/3$	91, 91'
$\theta = \tan^{-1} 4$	92, 92'
$\theta = \tan^{-1} 1/4$	93, 93'
$\theta = \tan^{-1} 2/3$	94 , 94'
$\theta = \tan^{-1} 3/2$	95, 95'
$\theta = \tan^{-1} 2/3$	96, 96'
$\theta = \tan^{-1} 3/2$	97, 97'
$\theta = \tan^{-1} 2/3$	98, 98'
$\theta = \tan^{-1} 2$	99, 99'
$\theta = \tan^{-1} 1/2$	100,100'
$\theta = \tan^{-1} 3$	101,101'

Angle of projection	Location of pixel that can be calculated
$\theta = \tan^{-1}1/3$	102, 102'
$\theta = \tan^{-1} 4$	103, 103'
$\theta = \tan^{-1} 1/4$	104, 104'
$\theta = \tan^{-1}3 /2$	105, 105'
$\theta = \tan^{-1}2/3$	106, 106'
$\theta = \tan^{-1}3/2$	107, 107'
$\theta = \tan^{-1}2/3$	108a, 108a'
$\theta = \tan^{-1}4$	108 , 108'
$\theta = \tan^{-1}1/4$	109, 109'
$\theta = \tan^{-1}3/2$	110, 110'
$\theta = \tan^{-1} 2/3$	111, 111'
$\theta = \tan^{-1}2$	112, 112'
$\theta = \tan^{-1} 1/2$	113, 113'
$\theta = \tan^{-1} 4$	114, 114'
$\theta = \tan^{-1}1/4$	115, 115'
$\theta = \tan^{-1}3$	116, 116'
$\theta = \tan^{-1}1/3$	117, 117'
$\theta =\tan^{-1}4$	108, 108'
$\theta =\tan^{-1}4$	119, 119'
$\theta = \tan^{-1}1/4$	120, 120'
$\theta = \tan^{-1}3$	121, 121'
$\theta = \tan^{-1} 1/3$	122, 122'

Angle of projection	Location of pixel that can be calculated
$\theta = \tan^{-1} 4$	123, 123'
$\theta = \tan^{-1} 1/4$	124, 124'
$\theta = \tan^{-1}3 /2$	125, 125'
$\theta = \tan^{-1}2/3$	126, 126'
$\theta = \tan^{-1}2$	127, 127'
$\theta = \tan^{-1}1/2$	128, 128'
$\theta = \tan^{-1}3$	129, 129'
$\theta = \tan^{-1}1/3$	130, 130'
$\theta = \tan^{-1}4$	131, 131'
$\theta = \tan^{-1}1/4$	132, 132'
$\theta = \tan^{-1}4$	133, 133'
$\theta = \tan^{-1} 3$	134, 134'
$\theta = \tan^{-1}1/3$	135, 135'
$\theta = \tan^{-1}4$	136, 136'
$\theta = \tan^{-1} 3/2$	138, 138'
$\theta = \tan^{-1}2/3$	139, 139'
$\theta = \tan^{-1}2$	140, 140'
$\theta = \tan^{-1} 3$	141, 141'
$\theta = \tan^{-1}1/3$	142, 142'
$\theta = \tan^{-1}4$	143, 143'
$\theta = \tan^{-1} 4$	144, 144'

Angle of projection	Location of pixel that can be calculated
$\theta = \tan^{-1}1/4$	145, 145'
$\theta = \tan^{-1}3$	146 , 146'
$\theta = \tan^{-1}1/3$	147 , 147'
$\theta = \tan^{-1}4$	148 , 148'
$\theta = \tan^{-1}1/4$	149 , 149'
$\theta =\tan^{-1}3/2$	150, 150'
$\theta = \tan^{-1}2/3$	151, 151'
$\theta = \tan^{-1}3$	152, 152'
$\theta = \tan^{-1}1/3$	153, 153'
$\theta = \tan^{-1} 4$	154, 154'
$\theta = \tan^{-1} 4$	155, 155'
$\theta = \tan^{-1}1/4$	156, 156'
$\theta = \tan^{-1} 3$	157, 157'
$\theta = \tan^{-1}1/3$	158, 158'
$\theta = \tan^{-1}4$	159, 159'
$\theta = \tan^{-1} 1/4$	160, 160'
$\theta = \tan^{-1}3$	161, 161'
$\theta = \tan^{-1}1/3$	162, 162'
$\theta = \tan^{-1} 4$	163, 163'
$\theta = \tan^{-1} 2$	164, 164'
$\theta = \tan^{-1} 3$	165, 165'
$\theta = \tan^{-1}1/3$	166, 166'

Angle of projection	Location of pixel that can be calculated
$\theta = \tan^{-1}3/2$	167, 167'
$\theta = \tan^{-1}2/3$	168, 168'
$\theta = \tan^{-1}3$	169, 169'
$\theta = \tan^{-1}1/3$	170, 170'
$\theta = \tan^{-1}2$	171, 171'
$\theta = \tan^{-1}1/2$	172, 172'
$\theta = \tan^{-1}3$	173, 173'
$\theta = \tan^{-1} 3$	174, 174'
$\theta = \tan^{-1} 1/3$	175, 175'
$\theta = \tan^{-1}4$	176, 176'
$\theta = \tan^{-1} 2$	177, 177'
$\theta = \tan^{-1}1/2$	178, 178'
$\theta = \tan^{-1}2$	179, 179'
$\theta = \tan^{-1}2$	180, 180'
$\theta = \tan^{-1}2$	181,

Chapter 6

Identification of components of h-v convex canonical discrete set with projections having angles θ = $\tan^{-1}2$, $\tan^{-1}1/2$, $\tan^{-1}3$, $\tan^{-1}1/3$ and reconstruction of the discrete set .

Our aim is to reconstruct the discrete sets with the existing above projections. So if the expected discrete set is hv-convex canonical, it is required to identify each components so that pixel value of individually component can be found out easily.

There are different canonical discrete set as per the pixel value of components at the touching points.

1	0	0	0	0	0	0	0	0	0
0	1	1	0	0	0	0	0	0	0
0	1	0	0	0	0	0	0	0	0
0	0	0	0	1	1	0	0	0	0
0	0	0	1	1	0	0	0	0	0
0	0	0	0	0	0	1	1	0	0
0	0	0	0	0	0	0	1	1	1

Fig – 13 (a)

6.1 Different cases of touching points between components

(1) At location A, the two connected pixel values of the components are all 1.The neighboring conjugate rays value of touching points are 1.

(2) At location C, the connected two pixel values are 0 and 1, the neighboring rays values of the touching point are also '0' and '1' .

(3) At location B, the all two pixels of connected point of components values are all 0. The neighboring conjugate rays values of touching point are also 0.

(4) If two pixels of connected point of components values are either 1, 0 or 0 ,0 and also it's neighboring pixel values are also 0, three or more conjugate rays value are 0.This is shown in the figure 13(b).

For getting touching points those should dealt differently.

1	0	0	0	0
0	DO	0	0	1
0	0	0	0	1
0	0	0	1	1
0	1	1	1	0

Fig – 13 (b)

6.2 Size of rays, pixels and equations of lines and solution of cases .

First consider the size of each pixel value is 1*1.

For projection $\theta = \tan^{-1}2$ for convenience the size of rays should be such that it cover 1/2 of the pixel of upper side.

For projection $\theta = \tan^{-1}1/2$ each ray cover the 1/2of the pixel of left side.

For projection $\theta = \tan^{-1}3$ for convenience the of rays should be such that it cover 1/3of the pixel of upper side.

For projection $\theta = \tan^{-1}1/3$ each ray cover the 1/3 of the pixel of left side .It is also shown on the figure 14.

As shown in the figure-14, O is the (0,0) coordinate. The 'x' coordinate and 'Y' coordinate are also shown.

We may consider here the left side of first ray as the first line. Similarly the left side of the second ray as the second line. The equations of different lines are given below.

(i). For projection $\Theta = \tan^{-1}2$

$Y = 2*X - (n1 - 1)$; where n1 is the line number.

(ii) For projection $\Theta = \tan^{-1} ½$

$Y = X/2 - (n2-1)/2$ .Where n2 is the line number.

(iii) For projection $\Theta = \tan^{-1}3$

$Y = 3*X - (n3 - 1)$; where n3 is the line number.

(iv) For projection $\Theta = \tan^{-1}1/3$

$Y = X/3 - (n4 - 1)/3$; where n3 is the line number

Projection of different angles with their rays (Fig-14

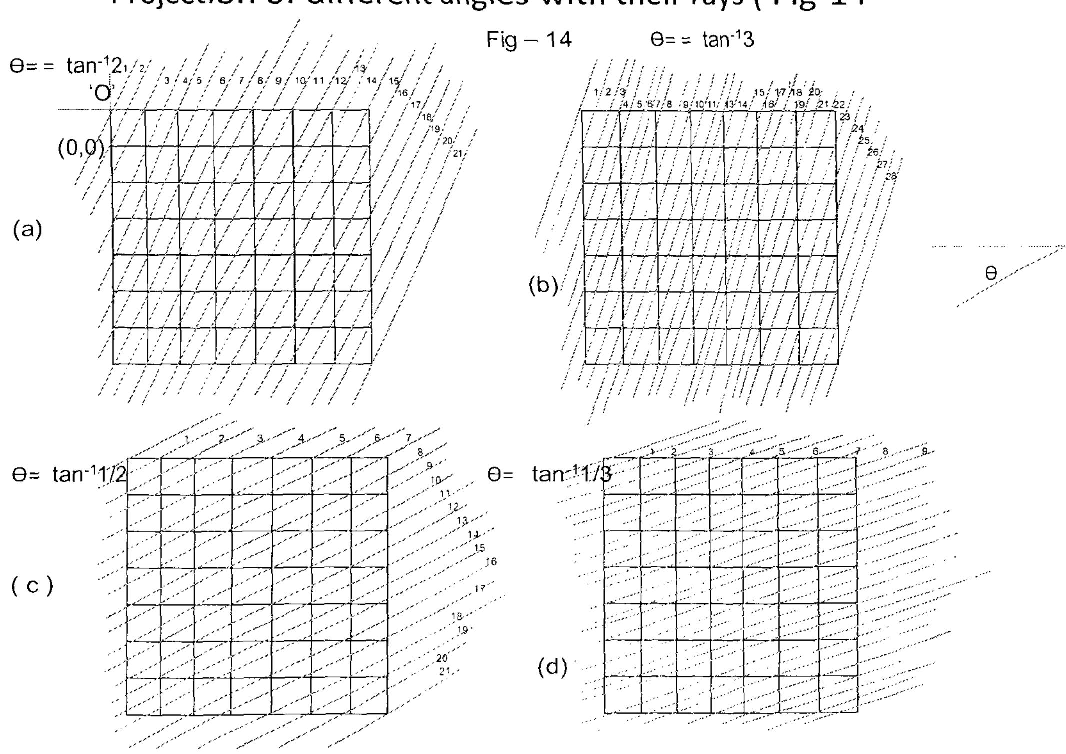

solution

For case (1) :

If it is found that in different projection angles if two conjugate rays values are found to be 1, Like rays (n-1) and n then line n should be consider .

Then we will have to find out the inter crossing points of above lines having coordinate values are integer numbers for

(i) for projection angle $\Theta = \tan^{-1}2$ and $\Theta = \tan^{-1}1/2$ and another for

(ii) for projection angle $\Theta = \tan^{-1}3$ and $\Theta = \tan^{-1}1/3$.

Then if find that the points of (i) is equal to the points of (ii ,)then these are the point of touching of the component. Then arrange those points in increasing order. If points are(X1, Y1), (X2,Y2) and (X3,Y3).Then this will appear as (x1<x2<x3) and (y1<y2<y3).

Then we get the component as (1 to X1) * (1 to Y1), (X1+1 to X2)*(Y1+1 to Y2)..

For case (2) :

This is the similar case of case (1), except we will have to consider the values of conjugate rays having values either (0,1) or (1,0).

For case (3) :

This is the similar case of case (1) , except we will have to consider the values of conjugate rays having values either (0 , 0) or (0 , 0) .

Case (iv) In this case it is found that in different projection angles more conjugate rays values are found to be 0 as shown in the figure. So there may many points due to these rays those satisfy the conditions of touching points.

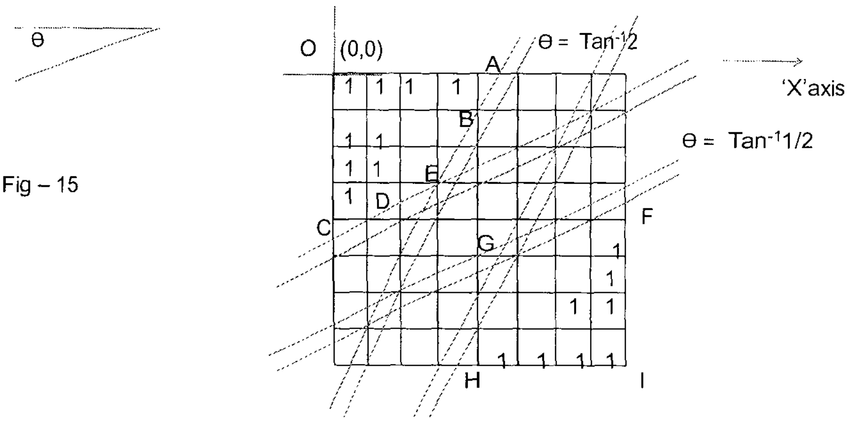

Fig – 15

Let the line of rays in ascending order be L1,L2 ,L3 etc for projection $\Theta = \text{Tan}^{-1}1/3$ .. Where L1 is the first line encounter the condition. Let the points those satisfy those conditions are

(X1 , Y1), (X2,Y2),.. ..(Xi ,Yi), ..(Xn , Yn). Here If the point of touching of components is (Xp , Yp), then the point should satisfy the condition. The is Xp<ceil(L1/3) and Xi< ceil(L1/3) and (Xi<Xp), where Xi and Xp are the x coordinate of any two of above points . .

Note : As in above figure it is not necessary to find the dimension of the components . To find pixel value of the discrete set we can consider the area OABEDC and FGHI. The pixel values of this area can be found out as per the procedure explained earlier.

6.3 :Ambiguity

cases : 1

There are some ambiguity cases in detecting the touching point . As in the figure it is given That ‘O’ is the actual touching point . But both ‘O’ and ‘A’ are found to be touching points .

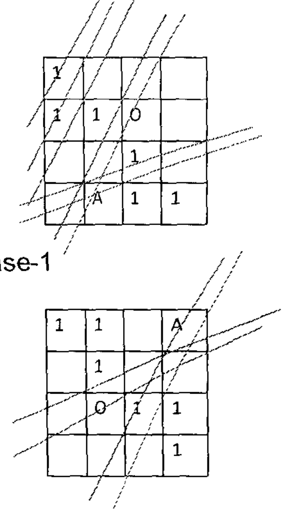

Case-1

case-2

Fig – 16

Actual point ‘Y’ axis is even point

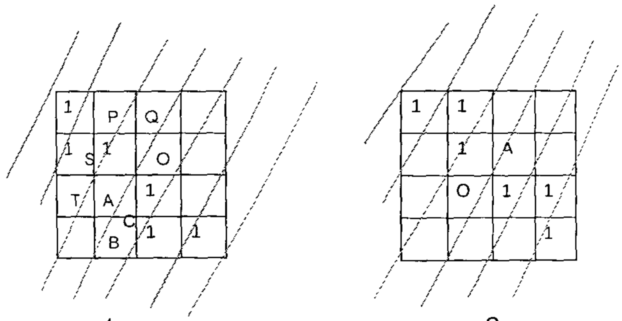

case-1 case -2

Detection of actual point

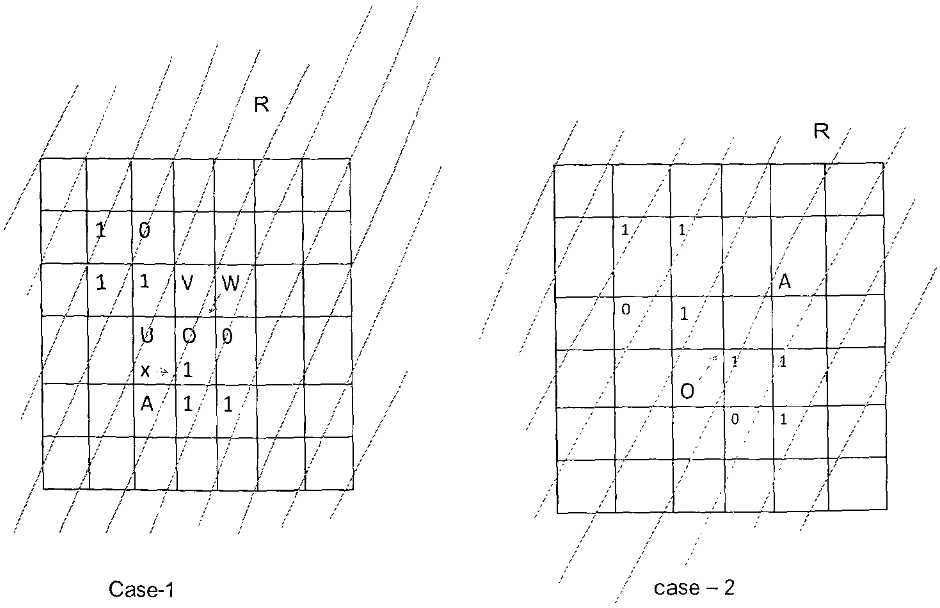

Case-1 case – 2

Detection of actual point in case of ‘Y’ axis is odd point

Detection of actual points In this case consider two rays as one ray. As 1&2 as one ray, and 3 & 4 as another ray and so on. The two points those are found, one have 'Y' coordinate even another have 'Y' coordinate is odd. The odd 'Y' coordinate point remain middle of the assumed ray where as the even coordinate point touches the edge. Here we have consider the rays having projection angle to be

$\Theta = \tan^{1}2$ and $\Theta = \tan^{1}1/2$

There are two cases one is odd 'Y' coordinate and another is even 'Y' coordinate. Let us consider the constant of the pixel that depend upon the actual pixel value is 'k' considering all pixels to be uniform and those represent '1' in binary image.

Then following observation is found.

(i) If 'Y' coordinate of actual point is odd,

The as per figure the ray cover the area of pixel having value '1' is

UVO +OWX = A/2 .

So the ray value is = (A/2)*A *K = K/2

(ii)If 'Y' coordinate of actual point is even. Then the area of the pixel having value 1 covered by the ray R is (3/4)*A or A.

So the ray value = (3/4)*(A/A)*K = (3/4)*k or k. So detection of points can be done as given below.

(a) When the ray's value is found to be (K/2) then the point having 'Y' coordinate odd is the actual point.

(b) When the ray's value is found to be (3/4)*k or A then the point having 'Y' coordinate even is the actual touching point.

Cases :2 In the figure it is shown that though B and C are the actual touching point but as per the algorithm A is also detected as the touching point. When we find that between any two partition points (Xi, Yi) and (Xj, Yj),
if ((Xi>Xj)&(Yi<Yj)) or ((Xi<Xj)&(Yi>Yj) then we conclude that ambiguity has occurred.

Way of detection of actual point :

In this case the all projection lines of all the points those does not satisfy the condition (Xi<Xj) and (Yi<Yj) are to be verified. If the line numbers of a point is equal to any other minimum two touching point's line numbers or neighbor line numbers with the condition that If Li,Lj ,Lk are the lines of points (Xi,Yi),(Xj,Yj) ,(Xk,Yk) then(Xi<Xj<Xk) and(Yi<Yj<Yk) and(Li<Lj<Lk) corresponding to their projection angles. Then that point is a ambiguous point.

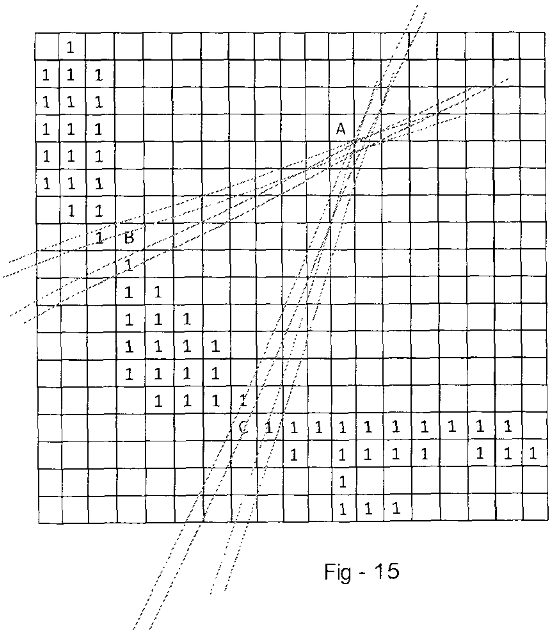

Fig - 15

6.4 Time complexity (worst case)

According to [3] the time complexity for reconstructing canonical hv-convex discrete sets is $O(m^3n^3.\min\{m^2,n^2\})$.

(i)Maximum number of lines in case of $\Theta = \tan^{-1}2$ & $\Theta = \tan^{-1}1/2$ is max(2*m +n,2*n + m)

(ii)Maximum number of lines in case of $\Theta = \tan^{-1}3$ & $\Theta = \tan^{-1}1/3$ is max(3*m +n,3*n + m)

Time complexity for finding crossing points of lines between projection (a) $\Theta = \tan^{-1}2$ & $\Theta = \tan^{-1}1/2$ and (b) $\Theta = \tan^{-1}2$ & $\Theta = \tan^{-1}1/2$ those are integer number is $O(m . n)$.

Time complexity of finding the points those in case of (a) equal to those in case of (b) is $O(m^2n^2)$ .Time complexity for rectification of ambiguity is $O(m^2n^2)$.

So worst case time complexity is $O(m^2n^2)$.

m = number of rows of the matrix and n = number of column of the matrix.

Chapter 7

Conclusion and Future Work

In this thesis we have shown that the components of any discrete set can be reconstructed without ambiguity by choosing suitable projection angles. Thus would be useful in computerized tomography.

It is also shown that the time complexity of reconstruction is less than those known earlier.

Further reduction of X-ray exposed area may also be possible if this method is applied to a special class of discrete sets, which satisfy some geometrical properties.

Reference :

1. Avinash C . Kak and Malcolm Slaney, Principle of Computerized Tomographic imaging, 2001.

2. Lee W. Goldman, Journal of Nuclear Medicine Technology, Volume 35, Number 3, 2007 115-128.

3. Peter Balazs, Reconstruction of Canonical hv-convex Discrete Sets from Horizontal and Vertical Projections. IWCIA 2009, LNCS 5852. pp. 280 288, (2009)

4. Lee W. Goldman, Principle of CT : Radiation Dose and Image Quality, J Nucl Med Technol 2007; 35:213-225.

(5) Peter Balazs, On the Ambiguity of Reconstructing hv-Convex Binary Matrices with Decomposable Configurations. Acta Cybernetica 18(2008) 367-377.

(6) Woeginger. G. W. The reconstruction of polyominoes from their orthogonal projections,Inform . Process .Lett, 77, 225-229(2001).

(7) Barcucci, E., Des Lungo, A., Nivat, M., Pinzani, R.: Reconstructing convex Polyminoes from horizontal and vertical projections. Theor. Comput. Sci . 155, 321 -347 (1996) .

(8) Brunetti, S.,Del Lungo, A., Del Ristoro, F., Kuba, A., Nivot, M.: Reconstruction of 4 and 8- connected convex discrete sets from row and column projections. Len Algebra Appl. 339, 37 57 (2001)

(9) Chrobak, M., Diirr, C. : Reconstructing hv- Convex polyminoes from orthogonal projections. Inform. Process. Lett. 69, 283 -289(1999)

(10) Kuba, A.:Reconstruction in different class of 2D discrete sets .in: Bertrand,. G., Couprie, M., Perroton, L. (eds) DGCI 1999. LNCS, vol .1568 , pp. 153 -163 . springs , Heidelberg (1999)

(11)Balogh, E., Kuba, A., Devenyi, C., Del Lungo, A.: comparison of algorithms for reconstructing hv-vonvex discrete set. Lin. Alg. Appl. 399, 23- 35 (2001)

(12) Barcucci,E.,Del Lungo, A., Nvat, M., inzani, R : Reconstructing convex polyominoes from horizontal and vertical projections. Theor Comput Sci. 155, 321 -347 (1996)

(13) Chrobak, M., Diirr, C.: Reconstructing hv convex polyominoes from orthogonal projections. Inform.Process Lett. 69, 283 -289(1999)